

Classical infrared spectra of ionic crystals and their relevance for statistical mechanics

Andrea Carati^a Luigi Galgani^a Alberto Maiocchi^a
Fabrizio Gangemi^b Roberto Gangemi^b

November 6, 2018

Abstract

It was recently shown that the experimental infrared spectra of ionic crystals at room temperature are very well reproduced by classical realistic models, and here new results are reported on the temperature dependence of the spectra, for the LiF crystal. The principal aim of the present work is however to highlight the deep analogy existing between the problem of spectra in ionic crystal models on the one hand, and that of energy equipartition in the Fermi–Pasta–Ulam model, on the other. Indeed at low temperatures the computations of the spectra show that the dynamics of the considered system is not completely chaotic, so that the use of the Boltzmann–Gibbs statistics is put in question, as in the Fermi–Pasta–Ulam case. Here, however, at variance with the equipartition problem, a first positive indication is given on the modifications that should be introduced in a classical statistical treatment: the new results at low temperatures show that it is indeed the Clausius identification of temperature that has to be modified. In fact, at very low temperatures the theoretical spectra fail to reproduce the experimental ones, if the temperature is taken as proportional to mean kinetic energy, but agreement is recovered through the only expedient of introducing a suitable temperature rescaling. Analogous results are also found in connection with thermal expansion.

Keywords: Infrared spectra, equipartition principle, ordered and chaotic motions, ionic crystal model, FPU model

^aDep. Mathematics, Università degli Studi di Milano, Via Saldini 50, 20133 Milano – Italy.

^bDMMT, Università di Brescia, Viale Europa 11, 25123 Brescia – Italy.

1 Introduction

The present paper reports new results concerning classical theoretical estimates of infrared spectra of ionic crystals. In two previous papers (see [1] and [2]) the estimates were given for spectra at room temperature, and here the temperature dependence of the estimates is investigated, particularly at low temperatures, for the Lithium Fluoride (LiF) crystal.

Thus stated, the problem seems to be one of interest for solid state physics, which indeed is the case. However, in this paper it is pointed out that we are actually meeting here with quite general problems of statistical mechanics. First of all, we are meeting with the problem of the relations between quantum statistical mechanics and its classical counterpart, if not between quantum and classical physics altogether. Because the theoretical spectra discussed here reproduce well the experimental data, as shown by Fig. 1 and 2 (for the LiF crystal at room temperature), while they are computed in purely classical terms involving solutions of Newton equations for the ions' motions, with no reference at all to energy levels and corresponding jumps.

Furthermore, we are meeting with a problem concerning the dynamical foundations of classical statistical mechanics. Indeed it will be seen that, as temperature is diminished, the dynamics of the considered model becomes less and less chaotic, so that the use of the Boltzmann–Gibbs statistical mechanics becomes less and less justified, as in the FPU case. On the other hand, a first positive indication is also provided here, because it is shown that what should be modified in a statistical treatment, is the Clausius identification of temperature T in terms of mean kinetic energy $\langle K \rangle$, namely, the relation

$$\langle K \rangle = \frac{3}{2} N k_B T , \quad (1)$$

where N is the number of particles and k_B the Boltzmann constant. Indeed it will be seen that, using the Clausius identification, at low temperatures the theoretical spectra fail qualitatively in connection with a certain feature of the spectrum. However, agreement is recovered if, at each of the two low temperatures considered (85 K and 7.5 K), the initial data are taken at a suitable value of the mean kinetic energy, which, through the Clausius identification, would correspond to a much larger “effective temperature” (180 and 125 K respectively). Analogous results are also obtained in connection with the thermal expansion.

The plan of the paper is as follows. In section 2 we illustrate some general features concerning realistic ionic crystal models, in particular how

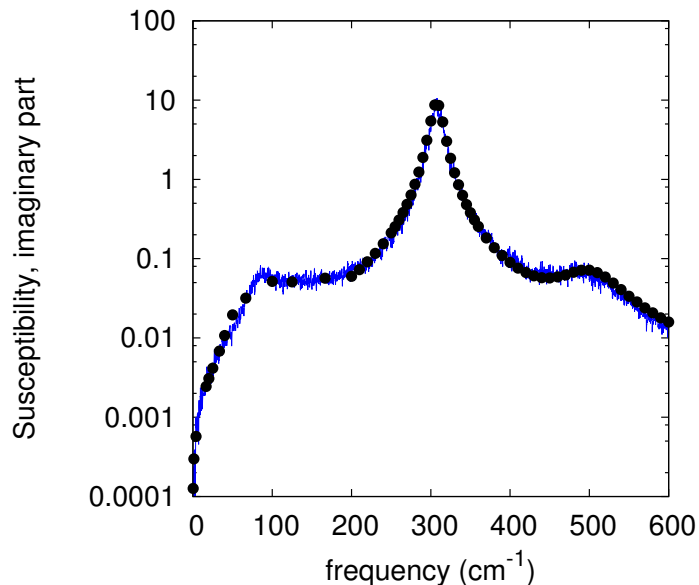


Figure 1: Imaginary part of susceptibility vs frequency, at room temperature. Comparison between calculations (solid line) and experimental data taken from [3] (points). Here, as in all following figures but Fig. 7, the computations are performed at a kinetic energy proportional to temperature according to the Clausius identification (1).

they can be considered as evolutions of the FPU model, and how ionic spectra can be dealt with in a classical statistical mechanical frame. In section 3 we give details on the concrete model used for the LiF crystal actually investigated. In section 4 we report the results on the spectra. First, results at room temperature which extend previous ones, and then their temperature dependence. Some comments are finally given in section 5. In an appendix some details are given concerning the determination of the parameters of the model, making use of the dispersion relations.

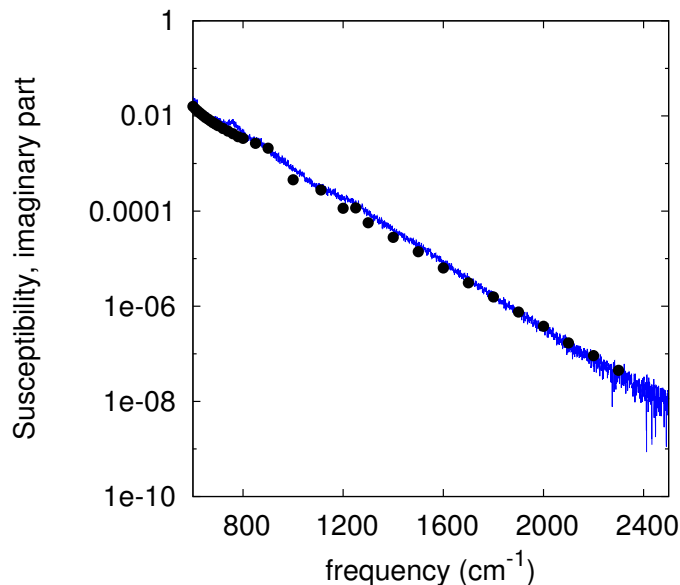


Figure 2: High frequency behavior of the imaginary part of susceptibility vs frequency (at room temperature) compared with experimental data.

2 Realistic ionic crystal models as evolutions of the FPU model. Classical infrared ionic spectra

It is well known that the FPU work put in question the applicability of the Boltzmann–Gibbs statistics in connection with the equipartition principle, for dynamical systems that don't present sufficiently chaotic motions. Now, the failure of the equipartition principle was observed in the FPU model, which is a simple, idealized model of a one-dimensional crystal. So it is not clear whether the FPU critique applies to concrete physical systems. On the other hand, a simple natural generalization of that model exists which emulates real systems, actually, ionic crystals. Moreover, ionic crystals are endowed with dielectric properties, so that they present optical spectra, which is a further physical phenomenon, perhaps the most characteristic one of quantum physics, that they allow to investigate.

Ionic crystals are known to be the simplest type of crystals (see [4][5]). For such crystals, as for the covalent ones, the degrees of freedom of the electrons can be eliminated, inasmuch as the electrons don't move around the crystal, but remain trapped, each about its own ion. Thus, at least for what concerns certain physical phenomena, the crystal can be reduced to a system of ions. Indeed, it was shown by Born (and proved later with quantum mechanical methods – see for example [6]) that the electrons can just be assumed to produce on the ions two effects: first, to endow each ion with a suitable "effective charge" entering the mutual Coulomb forces (thus emulating the ions' polarizability), and, second, to produce a further mutual repulsive "effective short-range force" among pairs of ions. Born himself suggested for the potential of the short-range force, the form $V^{(s)}(r) = a/r^6$, which involves only one free parameter. Other more sophisticated effective potentials were afterwards proposed, one of which was used in our model. The paradigmatic ionic crystal is that of LiF, which plays for crystals a role analogous to that of Hydrogen atom for atomic gases.

At this point, having eliminated the electrons, the ionic crystal model appears as a natural generalization of the FPU model, namely, as a system of point particles oscillating about the sites of a regular lattice, interacting through mutual two-body forces, which can be studied in terms of normal modes referred to the minimum of the potential energy. This was actually done in the year 1912 by Born and von Kármán [7] who, considering a model with two alternating masses, could highlight the distinction between acoustic and optical modes. Such a purely mechanical model, in its one-dimensional version, became a prototype for studies in perturbation theory related to the FPU model (see[8]), and is presently investigated in the thermodynamic limit within the modern statistical approach (see [9]), along the lines of [10] and [11]. However, any realistic model of a ionic crystal has to take into account also its dielectric properties, which are described in terms of ionic polarization. This is given by

$$\mathbf{P} = \frac{1}{V} \sum_{\mathbf{h},s} e_s \mathbf{q}_{s,\mathbf{h}} , \quad (2)$$

where $\mathbf{q}_{s,\mathbf{h}}$ is the displacement of ion s in cell \mathbf{h} from its equilibrium position, e_s its electric charge, V the volume. In this way infrared spectra enter the game.

Optical spectra are thermodynamic properties of a system, just as heat capacity and compressibility, which in statistical mechanical terms are defined as responses to changes of an external parameter, here the electric field.

Optical spectra actually show up as *spectral curves*, namely, functions which give the refractive index $n(\omega)$ versus frequency, or the reflectivity $R(\omega)$ and so on. All these are amenable to the curve $\chi(\omega)$ of electric susceptibility, or more precisely of the corresponding tensor $\chi_{ij}(\omega)$ in the crystal case.

The statistical mechanical expression for dielectric susceptibility took a rather long time to be established, actually up to the end of the years fifties, when linear response theory became available. Some papers by Gordon (see [12]) reconstruct the rather painful path that had to be followed. Starting from Schrödinger perturbation theory for estimating probabilities of energy jumps, and then passing to the Heisenberg picture, it was finally realized that the statistical mechanical susceptibility formula can be expressed in terms of essentially the time–autocorrelation function of polarization, the latter being a microscopic quantity which, for the aims of infrared spectra, involves the positions of the ions only. Such a formula is just a standard Green–Kubo one, which can be deduced also in a purely classical frame (see [13]), and more precisely has the form

$$\chi_{ij}^{ion}(\omega) = \frac{V}{\sigma_p^2} \int_0^{+\infty} e^{-i\omega t} \langle P_i(t) \dot{P}_j(0) \rangle dt . \quad (3)$$

Here $\langle \dots \rangle$ denotes ensemble average, P_j the j -th component of the ionic polarization \mathbf{P} given by (2), and σ_p^2 is a constant that reduces to $1/\beta$, if the average is performed using the Gibbs ensemble. In this case the formula takes the form

$$\chi_{ij}^{ion}(\omega) = \frac{V}{k_B T} \int_0^{+\infty} e^{-i\omega t} \langle P_i(t) \dot{P}_j(0) \rangle dt , \quad (4)$$

Anyhow, the ionic electric susceptibility turns out to be expressed in terms of essentially the time–autocorrelation function of the ionic electric polarization, a fact whose relevance will be pointed out below.

The contribution of electrons to the total susceptibility tensor χ_{ij} in the infrared amounts to a constant, which can be conveniently written as $(\epsilon_\infty - 1)/4\pi$, so that the electric permittivity tensor, which is defined by $\epsilon_{ij} = \delta_{ij} + 4\pi\chi_{ij}$, takes the form

$$\epsilon_{ij}(\omega) = \epsilon_\infty \delta_{ij} + 4\pi\chi_{ij}^{ion}(\omega). \quad (5)$$

In the case of LiF, which will be considered in this paper, the susceptibility tensor, and so also the permittivity tensor, are known to be multiples of the identity, thus reducing to scalar quantities. This property shows up

also in the numerical computations, as already observed in Ref. [1]. Thus we take for χ one third the trace of the tensor χ_{ij} .

Having available the statistical formula for electric permittivity, one can eventually recover macroscopic optical quantities such as refractive index n and reflectivity R , which are given (see [14]) by

$$n = \sqrt{\varepsilon} , \quad R = \left| \frac{\varepsilon - 1}{\varepsilon + 1} \right| .$$

The statistical mechanical formula (4) for electric susceptibility is the clue for the possibility itself of a purely classical approach to spectral lines. The point is that in such a formula any reference to energy levels and jump probabilities completely disappeared, and the microscopic relevant quantity is the time derivative of essentially the autocorrelation of the electric polarization, which involves particles positions and momenta only. Now, the same features occur also in the corresponding quantum formula, in which however positions and momenta are Heisenberg noncommuting operators. Thus, within a quantum approach the classical formula (4) is just understood as the corresponding *classical approximation*, the advantage of which with respect to the quantum formula is only that it can be concretely estimated through numerical computations (i.e., through molecular dynamics (MD) simulations), the same technique of the old FPU paper. But the purely classical formula should just give a first approximation, to which suitable *quantum corrections* ought to be added, especially when working in a fully quantum regime.

Indeed, some discussions are available in the literature (see [15][16]), concerning the choice of the best quantum correction. However, Figs. 1 and 2 show that a simple naive implementation of the purely classical formula for a model of LiF crystal, reproduces quite well the experimental data at room temperature, i.e., well below the Debye temperature (which is estimated to be about 730 K for the LiF crystal), and thus in a deep quantum regime, with no need of any quantum corrections at all.

We now come to the relations between infrared spectra and chaoticity. The point is that in ergodic theory chaoticity can be defined as corresponding to mixing, which is a property entailing that the time–correlation functions of all pairs of dynamical variables vanish for sufficiently long times. Now, the infrared spectrum is proportional to the Fourier transform of essentially the time–autocorrelation of electric polarization, and so the form of the infrared spectrum is reflected in the chaoticity properties of the considered dynamical system. In particular, in the low–energy limit, characterized by non chaotic motions (actually almost periodic ones) a line spectrum (one in which the

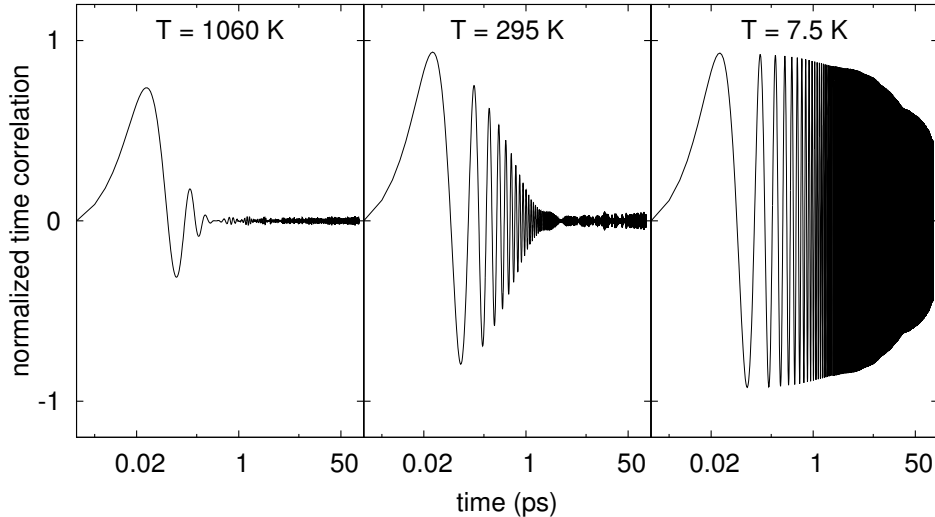


Figure 3: The normalized correlation function $\langle P_x(t)\dot{P}_x(0) \rangle$ vs time at three simulation temperatures: 1060, 295 and 7.5 K, from left to right. Here, P_x is the x component of electric polarization.

imaginary part of dielectric susceptibility is a sum of delta functions) is expected to occur. So the relevant correlation functions are expected to have relaxation times which increase, even possibly diverging, as temperature is decreased. To this end one can compute the time dependence of the time– correlation function $\langle P_x(t)\dot{P}_x(0) \rangle$, which can be conveniently normalized through division of $P_x(t)$ and $\dot{P}_x(0)$ by the corresponding standard deviations.

In Fig. 3 we report the results obtained for the LiF model studied in the present research, at three temperatures (defined through the Clausius identification), namely, 1060, 295 and 7.5 K. One clearly sees that at the two higher temperatures 1060 K and 295 K decorrelation essentially occurs at 0.1 ps and at 1 ps respectively, whereas at 7.5 K decorrelation doesn't occur at all even at 100 ps, and much longer times seem to be required. This fact already indicates that some caution is necessary in applying the standard methods of classical statistical mechanics at low temperatures. A preliminary study of the decay time of the relevant correlation as a function of temperature seems to hint at the existence of different laws for high and low temperatures. This is a point that we plan to better study in a future

work. The main goal of the present work is however to concentrate on the form of the infrared spectra at low temperatures.

3 The LiF crystal model

The calculation of infrared spectra is reduced, as recalled above, to generating classical orbits of the ions and performing suitable ensemble averages. We accomplish this task by running MD simulations for a LiF crystal model.

As in Ref. [1], we represent the crystal as a system of N point particles, with the masses of Li and F ions taken from experiment. The interactions among the particles are described by a two-body potential V , which includes both the Coulomb term and a short range effective potential $V^{(s)}$,

$$V(r_{ij}) = \frac{e_i e_j}{r_{ij}} + V_{ij}^{(s)}(r_{ij})$$

where indices i, j denote the atomic species, Li or F, and $e_i = \pm e_{eff}$.

For the short range effective potential, instead of the simple form $V^{(s)}(r) = a/r^6$ proposed by Born and used in Ref. [1], the so-called Buckingham potential

$$V_{ij}^{(s)}(r) = A_{ij} \exp(-B_{ij}r) - \frac{C_{ij}}{r^6}$$

is adopted here.

A cubic simulation cell together with periodic boundary conditions is used: long range electrostatic interactions are calculated by means of a standard Ewald summation procedure, while for the short-range effective forces a 5 Å cut-off is applied.

The size of the simulation cell should be chosen at each temperature in order to match the experimental density of the crystal (at ordinary pressure). At room temperature we take for the lattice step the experimental value, i.e., 2.01 Å as we did in Ref. [1]. At different temperatures, instead, we adjust the size of the simulation cell in such a way that the calculated primary peak shifts in accordance with the experimental observations. As will be discussed in detail later in connection with thermal expansion at low temperatures, this procedure is pretty well compatible with the experimental data for density.

Besides the lattice spacing, we have to fix the parameters of the potential, namely, the effective charge e_{eff} and the coefficients A_{ij}, B_{ij}, C_{ij} of the short range interaction. To fix these parameters, we first of all require that the stable equilibrium position of the system corresponds to the LiF lattice, i.e., a FCC structure with two ions per cell, with the two ions species alternating

along the three orthogonal directions. In addition, a fit is made between the computed dispersion relations and the experimental ones; this is explained in the Appendix. The parameters used (the same for all temperatures) are reported in Table 1.

Finally, the choice of the parameter ε_∞ is done as follows. Since the highest frequency we can reach, due to size of the integration step, is about 8000 cm^{-1} , we require that Eq. (5) matches, at such a frequency, the experimental value taken from Ref. [3]. In such a way, the value $\varepsilon_\infty = 1.92$ is obtained. The choice of this parameter strongly influences the decay of reflectivity on the side of high frequencies, and in particular a value lower than 1.92 would give a better agreement with the data. We however chose the value 1.92 which is in good agreement with the values reported in the literature for n_∞ of LiF (see Ref. [17]).

MD simulations are performed on a system of $N = 4096$ ions. Numerical integration of the equations of motion is performed at constant energy and constant volume, using the Verlet algorithm with an integration step of 2 fs.

A key point concerns the energy that should be used in each computation, namely, how should it be related to the experimental temperature T . We started our research using the procedure commonly employed in MD simulations, which fixes the initial mean kinetic energy $\langle K \rangle$ through the Clausius prescription (1). This can be achieved in several ways, and we just chose the most direct one, sometimes called the *a posteriori* method. Namely, in order to simulate the system at a temperature T through the corresponding kinetic energy K , the lattice is initially set at its equilibrium configuration, and the ions are given random velocities according to the Maxwell-Boltzmann distribution with a certain temperature parameter T_{in} (typically $T_{in} \simeq 2T$). After a short transient time of 1000 integration steps, the lattice temperature is calculated from the mean kinetic energy of the ions and, if it differs from its target value T by more than a threshold amount, the process is repeated with a rescaled initial parameter T'_{in} . When

	A (eV)	B (\AA^{-1})	C (eV $\cdot\text{\AA}^6$)
Li-F	$3.30 \cdot 10^3$	5.00	9.40
F-F	$15.8 \cdot 10^3$	4.44	41.6
Li-Li	$3.18 \cdot 10^3$	6.29	-2.77

Table 1: Optimized parameters of the short range potential with effective charge 0.7281 e.

the mean kinetic energy attains the desired value, the actual simulation is started up, usually with a duration of 200 ps.

Ensemble averages in Eq. (4) are replaced by a time average over the simulation time, but in order to increase the statistical significance of the results, multiple simulations (usually 10) are run for each case.

4 Results

We preliminarily checked the method by working at room temperature. The first two results concern $\text{Im } \chi$, the imaginary part of susceptibility. The first one concerns its trend near the main peak, which is reported in Fig. 1. This figure can be compared both with the results of our previous work Ref. [1], and with the old quantum estimates of Ref. [18, 19]. The improvement with respect to our results of Ref. [1] may be attributed to the larger number of parameters of the short range effective potential and to the fact that the parameters are optimized by fitting the dispersion relations. In particular the agreement with experiment obtained at the two shoulders is indicative of a rather satisfactory behavior of the non-linear part of the potential. An analogous improvement occurs also for the real part of susceptibility, not reported here.

The second result concerns the decay of $\text{Im } \chi$ for high frequencies. As is well known, the experimental data (see Ref. [20]) show that such a quantity becomes extremely small at large frequencies, displaying an exponential decay over six orders of magnitude. Thus $\text{Im } \chi$ becomes very small, and hard to estimate numerically in a reliable way (see for example Ref. [21], page 4873). This difficulty can be overcome, and in Fig. 2 the numerical results thus obtained are compared with the experimental data, exhibiting an impressive agreement over six orders of magnitude.

In the following lines, some technical details are discussed, concerning two sources of error that had to be taken into account. The first one is the loss of analyticity of the correlations, which has a direct impact on the exponential decay (as explained in Ref. [22]), and is due to the truncation of the integral (4) to a finite time domain. The second source is the fact that the time average is performed over a finite time domain, which implies that the correlations $\langle P_i(t)P_i(0) \rangle$ are not positive definite in the Bochner sense, as they have to be. Analyticity is recovered by using a suitable Gaussian filter. Instead, in order to minimize the distortions introduced by the finiteness of the time average in the computation of $\text{Im } \chi$, we perform the integration in (4) in a symmetric interval $[-t_f, t_f]$, by exploiting the parity property of the

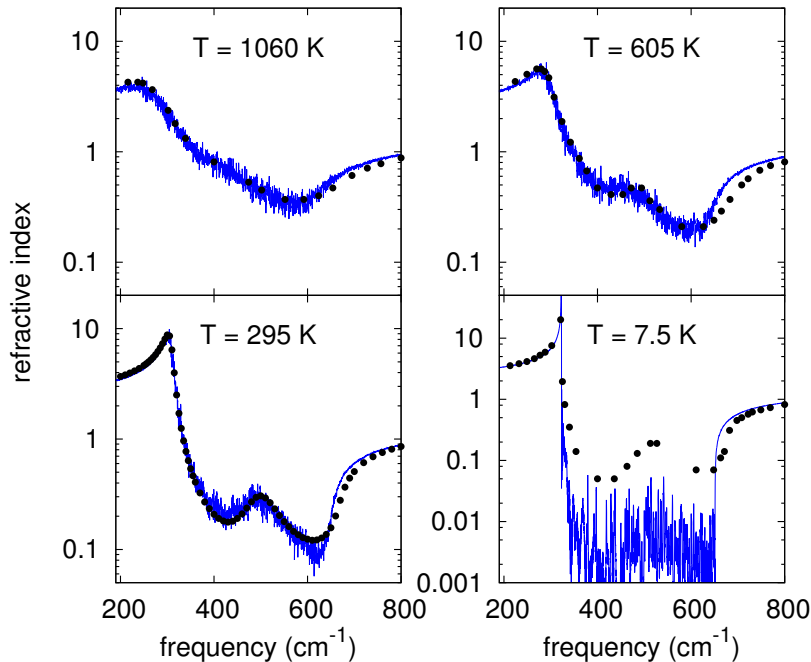


Figure 4: Calculated refractive index spectrum (solid lines) compared with experimental data [23] (full circles), at several temperatures.

correlations. Now, being known from theory that $\text{Im } \chi$ is positive for positive frequencies, we consider as unreliable the spectrum in the region where the computed values are negative, and this forces us to restrict ourselves to the domain $\omega < 2500 \text{ cm}^{-1}$.

In order to investigate the temperature dependence of the spectra, which is the main goal of the present work, we started considering the refractive index. In Fig. 4 the curves calculated at several temperatures are compared with the experimental data taken from Ref. [23].

Given the surprisingly good agreement of the classical spectrum with the experimental one at room temperature (295 K), which is a temperature lower than the Debye one (about 730 K for LiF), one may expect that the agreement should even improve at higher temperatures. In fact, at higher temperatures the calculated refractive index matches the data nicely. The spectra, sure enough, grow more noisy and the peaks broaden, as can be

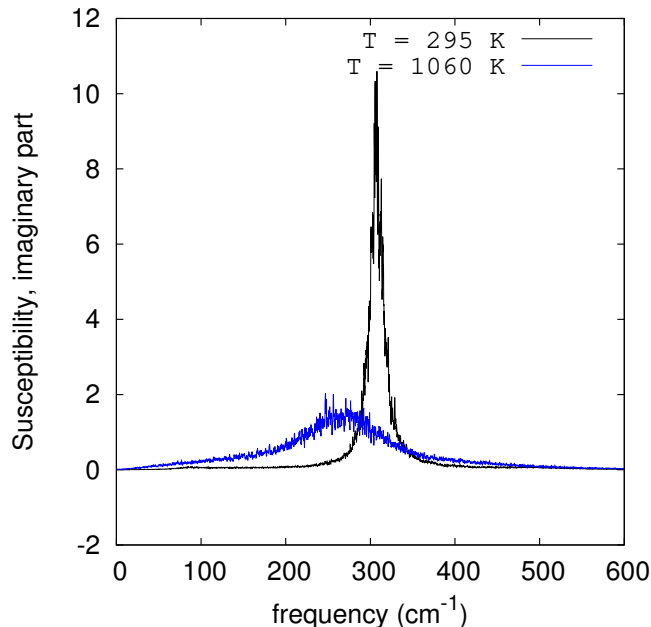


Figure 5: Calculated susceptibility spectrum (imaginary part) at room temperature and at 1060 K (near the melting point).

better appreciated by looking directly at the imaginary part of susceptibility (Fig. 5). This is obviously due to the nonlinearity, which increases as temperature is raised. The good agreement is a proof of the ability of our potential to reproduce the non-linear effects.

Instead, it is apparent that at 7.5 K the calculated spectrum substantially differs from the measured one in the region between 300 cm^{-1} and 600 cm^{-1} (notice the change of scale for the ordinates, at 7.5 K), where a secondary peak is present in the experimental data, but is absent in the numerical ones. Now, 7.5 K is just the temperature at which, as shown in Fig. 3 the relevant correlation did not yet decay, so that one may wonder whether the discrepancy would disappear by performing much longer computations exhibiting a full relaxation. It is clear however that with longer computations the discrepancy, rather than being eliminated, would even be enhanced. Indeed, dealing, as we are doing here, with an integral truncated at a certain time τ , we are actually performing a convolution between the “true” Fourier transform and the test function $(\sin \omega \tau)/\omega$. Now, the effect

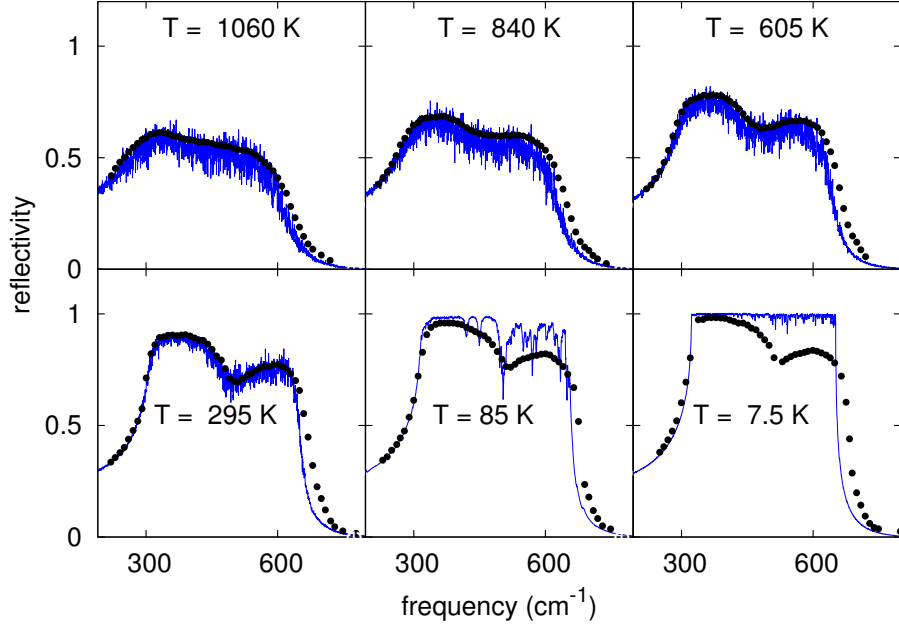


Figure 6: Calculated reflectivity spectra (solid line) compared with experimental data [24] (points) at several temperatures.

of such a convolution with respect to a “true” peak consists in smearing it out (and possibly adding some spurious peaks very near the original one). Thus, a truncation at a larger time $\tau' > \tau$ would essentially produce an analogous more pronounced peak but not a second one at a sensible distance. So, even if the correlation function were computed up to a much longer time, possibly attaining decorrelation, the computed spectrum would not reproduce the secondary peak exhibited by the experimental data. The main contribution of the present paper consists, as will be shown below, in pointing out that the remedy to this discrepancy is obtained through a qualitatively new expedient, which involves the identification of temperature in mechanical terms.

Concerning the discrepancy at 7.5 K, the relevant point is that the frequency of the secondary peak does not show up among the frequencies of

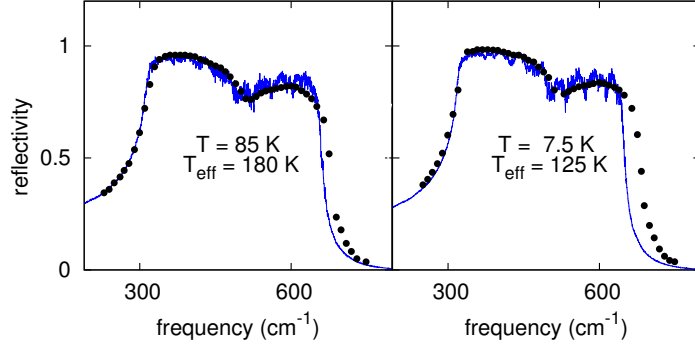


Figure 7: Calculated reflectivity spectrum (solid lines) compared with experimental data [24] (points) at low temperatures, with temperature rescaling. Here, T refers to experimental data, while T_{eff} is the rescaled value used in the computations.

the linearized system, so that its presence should be an effect of the nonlinearity. So an apparently contradictory situation occurs, because the nonlinearity decreases with decreasing energy, whereas in the experimental data the visibility of the secondary peak increases with decreasing temperature.

In order to better understand such a discrepancy, we decided to consider also reflectivity, for which a larger set of experimental data is available (see for example Ref. [24]), and which was studied since a long time (see [25]). Here one has to take into account that the feature under discussion, namely, the occurring of a secondary peak at about 500 cm^{-1} in the refractive index curves, manifests itself in the reflectivity curves as a hollow. The calculated reflectivity curves are reported, together with the experimental data, in Fig. 6. One sees that in the experimental spectra the hollow starts becoming visible at 840 K, and its visibility increases as temperature is lowered. Instead, the theoretical curves reproduce well the experimental ones only from the highest temperatures down to room temperature, because the hollow is poorly reproduced already at 85 K, and completely disappears at 7.5 K, where the reflectivity becomes essentially uniform, sticking at the value 1.

So, the experimental results concerning the secondary peak (or the hollow) seem to indicate that the nonlinearity does not vanish as the temperature goes to zero, i.e., that kinetic energy does not vanish at zero temperature.

Now, the nonvanishing of kinetic energy at zero temperature is nothing but the well known Debye–Waller effect which, in quantum mechanical terms, is just a manifestation of zero–point energy. On the other hand, in the present context in which the Boltzmann–Gibbs statistics is put in question due to the non complete chaoticity of the motions, the idea naturally presents itself that an analogue of zero–point energy might be introduced in a classical model too. By the way, in the literature it was already pointed out that quantum phenomena exist which can be emulated by classical computations performed at suitable “elevated” temperatures. See Refs. [26],[27], and [28], Fig. 2.

More concretely, having in mind the possibility of emulating zero–point energy, and without any presumption of introducing a theory, in the present context we first of all start abandoning the Clausius identification of temperature as proportional to mean kinetic energy. Then, with a very simple, pragmatic attitude, just by trial and error we look for two suitable values of the mean kinetic energy which, inserted in the initial data, may allow us to reproduce sufficiently well (if possible at all) the experimental spectra corresponding to 85 and 7.5 K. Such values of the kinetic energy can also be expressed in terms of “effective temperatures”, just meant as the temperatures that correspond to given kinetic energies through the Clausius prescription. In such a way, just by a lucky guess we found the surprising result that the spectra at 85 and 7.5 K are pretty well reproduced by classical computations at suitable effective temperatures of 180 and 125 K respectively, as shown by Fig. 7. This is indeed the main, unexpected result

T (K)	$a_0(\text{noresc})$	$a_0(\text{resc})$	$a_0(\text{exp})$
7.5	1.988	1.995	2.001
85	1.995	2.001	2.002
295	2.010	2.010	2.010
605	2.034	2.034	2.033
840	2.055	2.055	2.055
1060	2.073	2.073	2.078

Table 2: Lattice steps used to reproduce data at several temperatures. Second column: values used in our simulations with no rescaling; third column: values used in our simulations with rescaled temperatures; fourth column: values obtained by applying thermal expansion coefficient from Ref. [17] to the value at 295 K.

obtained in this paper.¹

Apparently the agreement at the two low temperatures, both in connection with the hollow and in general for the whole spectrum, is of the same quality as at the higher temperatures. True, some disagreement is observed at the right shoulder, but this occurs somehow at the same degree at all temperatures. The reason of this minor fact is not yet clear to us, and we hope to understand it in the future. Perhaps a simple explanation might be related to the choice of the parameter ϵ_∞ discussed in section 3.

A strictly related phenomenon involving temperature rescaling, actually just the same rescaling as for spectra, was met in connection with the lattice spacing. As explained in section 3, at all temperatures different from 295 K the calculated spectra are obtained by adjusting the lattice spacing in such a way that the position of the main peak matches experiment. The values of the lattice spacing found in this way, with and without temperature rescaling, are compared in Table 2 with those obtained from the experimental data available in the literature (see Ref. [17]) for the thermal expansion coefficient of LiF. The agreement above room temperature is impressive. At 85 and 7.5 K, instead, the agreement is not so good if temperatures are not rescaled: indeed a qualitative failure is found here, because the theoretical values continue to decrease almost linearly, while the experimental ones exhibit a saturation effect. After temperature rescaling, the value at 85 K perfectly agrees with the experimental one, while at 7.5 K there is still a little deviation, but much less than before. This behavior corresponds to the one found in the spectra, so that one is led to guess that the two effects stem from the same origin.

5 Conclusions

The results obtained are apparently interesting. Indeed, already the good agreement of the classical spectra with the experimental ones at room temperature, obtained in a previous work without invoking any energy quantization, might have been unexpected. But the fact that even at almost absolute zero the classical computations of the spectra reproduce well the experimental data through the only expedient of suitably rescaling temperature, all other purely classical ingredients remaining unchanged, appears to

¹By the way, it turns out that, at the considered effective temperature of 125 K, the relevant correlation actually decays to zero in about 10 ps. Thus the problem of the truncation time which arises at an effective temperature of 7.5 K (see Fig. 3) does not arise here.

be really surprising. Moreover, the impression that here one is not meeting with some fortuitous coincidence, is supported by the agreement found for thermal expansion too.

On the other hand it is well known that the Clausius identification of temperature with kinetic energy is in contrast with experiment, for example because zero-point energy in solids exists. This was indeed one of the main historical reasons for abandoning classical mechanics. Here, however, it has been also shown that, for what concerns infrared spectra, classical statistical mechanics is adequate if a suitable rescaling of temperature is introduced.

So the problem arises whether the Clausius identification of temperature is a necessary implication in classical statistical mechanics. Some comments are given here. A first question in this connection is whether temperature should be defined as the mean value of some observable, as is suggested by the Clausius identification of temperature with mean kinetic energy in the classical case. The question then becomes of understanding which quantity does a thermometer measure if it doesn't measure kinetic energy. On the other hand, we point out, at equilibrium temperature occurs, both in the classical and the quantum cases, as a parameter which enters the Gibbs distribution, determining the mean value of energy. However, the temperature defined in such a way turns out to be proportional to mean kinetic energy only in the classical case, while in the quantum case the relation between temperature and kinetic energy is not universal, and depends on the considered system.

So, not being the average of an observable, it is not clear how temperature should be defined² if the Gibbs ensemble is not justified, as occurs in classical statistical mechanics in lack of suitable ergodicity properties. This is indeed the problem that was raised by the FPU work, which pointed out that energy equipartition, the main consequence of classical statistical mechanics, does not occur at low energies for the simplest model of a crystal. Apparently, the same occurs in connection with the infrared spectra of ionic crystals.

A provisional conclusion, in our opinion, might be the following. The Clausius identification of temperature as mean kinetic energy in classical statistical mechanics seems not to be justified in cases, such as that of FPU-type models at low energies, where suitable ergodicity properties are not guaranteed. The general problem of how a statistical mechanics should be formulated in such cases then remains completely open, and actually is a formidable one. However the results illustrated here for a realistic FPU-type

²Apart from introducing a microscopic model of a thermometer.

model presenting dielectric properties, with their surprising agreement with experiment, seem to indicate that a general solution may exist.

Acknowledgments. The use of computing resources provided by CINECA is gratefully acknowledged.

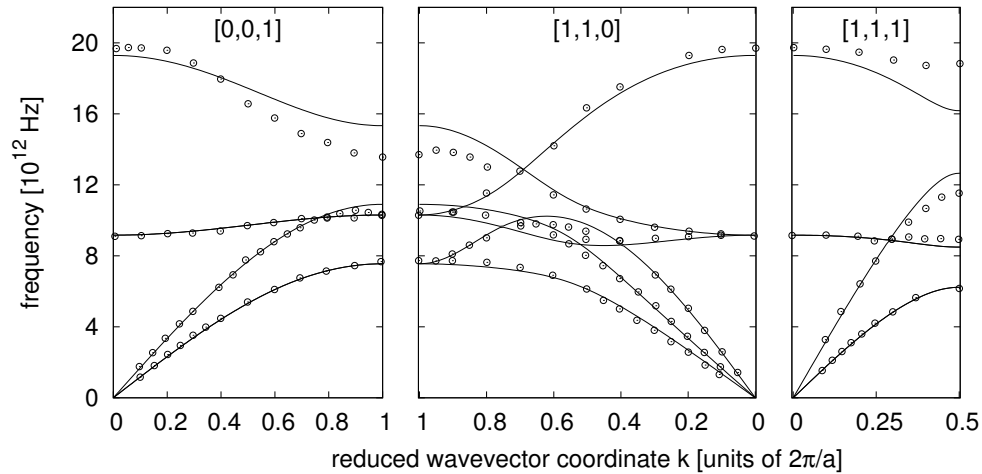


Figure 8: Solid lines: calculated dispersion relations. Circles: data from Ref. [29]

Appendix: fit of dispersion relations

The parameters of the potential are determined by comparison of calculated dispersion relations with experimental data taken from Ref. [29]. At variance with MD simulations, we consider an infinite crystal and linearize the model around the equilibrium positions, obtaining an infinite number of linear equations, with parameters which depend on the parameters of the potential. We then find the normal modes solutions for such equations, i.e., solutions in the form of travelling waves $\mathbf{q}_{s,\mathbf{h}} = \mathbf{Q}_s^{(l)} e^{i(\mathbf{k}\cdot\mathbf{x}_{\mathbf{h}} - \omega t)}$, thus determining the dispersion relations $\omega = \omega^l(\mathbf{k})$ for the different branches. Then we minimize the quantity $\sum_l \sum_i |\omega^l(\mathbf{k}_i) - \omega_i^l|^2$, ω_i^l being the experimental values at $\mathbf{k} = \mathbf{k}_i$, by varying the parameters of the potential. The best fit is shown in fig. 8 for the three high symmetry directions of the wave vector. In general there are three optical and three acoustical branches, two transverse

and one longitudinal for each group, with a possible degeneration in the transverse ones, depending on the direction of \mathbf{k} . The agreement with data, which is generally good for the acoustic branches and for the transverse optical branches, is not so satisfactory for some parts of the longitudinal optical branches, especially at high values of $|\mathbf{k}|$. This could be due to the absence of atomic polarizabilities in our model: indeed, much better results were obtained in Ref [29], where atomic polarizabilities were also taken into account in the model.

The optimized parameters we find are reported in Table 1.

References

- [1] F. Gangemi, A. Carati, L. Galgani, R. Gangemi, A. Maiocchi, Europhys. Lett. 110 (2015) 47003.
- [2] F. Gangemi, R. Gangemi, A. Carati, A. Maiocchi, L. Galgani, Europhys. Lett. 116 (2016) 37001.
- [3] E. Palik, Handbook of optical constants of solids, Academic Press, Amsterdam, 1998.
- [4] F. Seitz, The modern theory of solids, Dover, New York, 1987.
- [5] M. Born, K. Huang, Dynamical theory of crystal lattices, Clarendon Press, London, 1954.
- [6] H. Eyring, Quantum Chemistry, Wiley, New York, 1948.
- [7] M. Born, Th. von Kármán, Phys. Z. 13 (1912) 287.
- [8] L. Galgani, A. Giorgilli, A. Martinoli, S. Vanzini, Physica D 59 (1992) 334.
- [9] A. Carati, J. Stat. Phys. 128 (2007) 1057.
- [10] A. Maiocchi, D. Bambusi, A. Carati, J. Stat. Phys. 155 (2014) 300.
- [11] W. De Roeck, F. Huveneers, Pure Appl. Math. 68 (2015) 1532.
- [12] R. G. Gordon. J. Chem. Phys. 41 (1964) 1819.
- [13] A. Carati, L. Galgani, Eur. Phys. J. D 68 (2014) 307.
- [14] M. Born, Optik, Springer, Berlin, 1972.

- [15] R. Ramirez, T. López-Ciudad, P. Kumar, D. Marx, *J. Chem. Phys.* 121 (2004) 3973.
- [16] S. Bonella, M. Monteferrante, C. Pierleoni, G. Ciccotti, *J. Chem. Phys.* 133 (2010) 164104.
- [17] D.B. Sirdeshmukh, L. Sirdeshmukh, K. G. Subhadra, *Alkali Halides. A Handbook of Physical Properties*, Springer, Heidelberg, 2001.
- [18] A.A. Maradudin, R.F. Wallis, *Phys. Rev.* 123 (1961) 777.
- [19] R.F. Wallis, M. Balkanski, *Many-body aspects of solid state spectroscopy*, North-Holland, Amsterdam, 1986.
- [20] A. Kachare, G. Andermann, L.R. Brantley, *J. Phys. Chem. Solids* 33 (1972) 467.
- [21] P.H. Berens, K.R. Wilson, *J. Chem. Phys.* 74 (1981) 4872.
- [22] A. Carati, A. Maiocchi, *J. Opt. Soc. Am. A* 33 (2016) 1193.
- [23] H. H. Li, *J. Phys. Chem. Ref. Data* 5 (1976) 329.
- [24] J. R. Jasperse, A. Kahan, J. N. Plendl, S. S. Mitra, *Phys. Rev.* 146 (1966) 526.
- [25] M. Gottlieb, *J. Opt. Soc. Am.* 50 (1960) 343.
- [26] S. D. Ivanov, A. Witt, D. Marx, *Phys. Chem. Chem. Phys.* 15 (2013) 10270.
- [27] P. Kumar, D. Marx, *Phys. Chem. Chem. Phys.* 8 (2006) 573.
- [28] D. Marx, M. Parrinello, *Z. Phys D.* 41 (1997) 253.
- [29] G. Dolling, H. G. Smith, R. M. Nicklow, P. R. Vijayaraghavan, M. K. Wilkinson, *Phys. Rev.* 168 (1968) 970.